

Spin Control in Oxamato-Based Manganese(II)–Copper(II) Coordination Polymers with Brick-Wall Layer Architectures

Jesús Ferrando-Soria,[†] Jorge Pasán,[‡] Catalina Ruiz-Pérez,[‡] Yves Journaux,^{*,§} Miguel Julve,[†] Francesc Lloret,^{*,†} Joan Cano,[†] and Emilio Pardo^{*,†}

[†]Departament de Química Inorgànica, Instituto de Ciencia Molecular (ICMOL), Universitat de València, 46980 Paterna, València, Spain

[‡]Laboratorio de Rayos X y Materiales Moleculares, Departamento de Física Fundamental II, Universidad de La Laguna, 38201 La Laguna, Tenerife, Spain

[§]Institut Parisien de Chimie Moléculaire, Université Pierre et Marie Curie-Paris 6, UMR 7201, F-75252 Paris, France

S Supporting Information

ABSTRACT: Two new heterobimetallic manganese(II)–copper(II) coordination polymers of formulas $[\text{Mn}_2\text{Cu}_2(\text{Me}_3\text{mpba})_2(\text{H}_2\text{O})_6] \cdot 8\text{H}_2\text{O}$ (**1**) and $[\text{Mn}_2\text{Cu}_2(\text{Me}_4\text{ppba})_2(\text{H}_2\text{O})_6] \cdot 8\text{H}_2\text{O}$ (**2**) [Me_3mpba = 2,4,6-trimethyl-*N,N'*-1,3-phenylenebis(oxamate) and Me_4ppba = 2,3,5,6-tetramethyl-*N,N'*-1,4-phenylenebis(oxamate)] have been synthesized following a molecular-programmed self-assembly method from the corresponding dicopper(II) complexes acting as metalloligands toward Mn^{II} ions. **1** and **2** consist of neutral $\text{Mn}^{\text{II}}_2\text{Cu}^{\text{II}}_2$ layers with a brick-wall structure made up of oxamato-bridged $\text{Mn}^{\text{II}}\text{Cu}^{\text{II}}$ chains connected through double meta- (**1**) and para-substituted (**2**) permethylated phenylene spacers. Overall magnetic (**1**) and nonmagnetic (**2**) layer ground states result from the ferro- and antiferromagnetic interchain interactions between the oxamato-bridged $\text{Mn}^{\text{II}}\text{Cu}^{\text{II}}$ ferrimagnetic chains across *m*- and *p*-phenylene spacers, respectively. Interestingly, compound **1** exhibits a long-range ferromagnetic ordering with a rather high Curie temperature (T_C) of 20.0 K.

Ligand design plays a crucial role in the search for new examples of multidimensional coordination polymers showing interesting and predictable structures and magnetic properties,^{1–4} referred to as metal–organic polymers (MOPs). First, it allows one to gain control of the final dimensionality and topology of the MOP, and, second, it provides a way to efficiently transmit the magnetic interactions between the metal ions in a controlled manner. In this respect, the use of the so-called “complex-as-ligand” strategy, where a preformed precursor complex acts as a ligand (metalloligand) toward free paramagnetic metal ions, shows clear advantages against the more spread serendipitous self-assembly methods for the obtention of open-framework magnets, that is to say, molecular-based compounds combining both an open-framework two- (2D) or three-dimensional (3D) porous structure and spontaneous magnetization below a critical temperature (T_C).⁵

During the last years, our research group has succeeded in developing a new class of oxamato-based MOPs by means of molecular-programmed self-assembly methods based on ligand design.⁶ Along this line, our strategy consisted of using oxamato-based metallacyclic precursor complexes with predetermined

magnetic properties via the spin-polarization mechanism.⁷ For instance, two double-stranded dicopper(II) metallacyclophane precursor complexes, $[\text{Cu}_2(\text{mpba})_2]^{4-}$ and $[\text{Cu}_2(\text{ppba})_2]^{4-}$ [mpba = *N,N'*-1,3-phenylenebis(oxamate) and ppba = *N,N'*-1,4-phenylenebis(oxamate)] were successfully employed as effective ferro- and antiferromagnetic synthons, respectively, in the construction of a family of hexacopper(II) complexes with predictable magnetic properties.⁸ This strategy was subsequently extended to higher-dimensionality MOPs.⁶ Thus, $[\text{Cu}_2(\text{mpba})_2]^{4-}$ acting as a tetrakis(bidentate) metalloligand toward bis(chelated) Co^{II} ions yielded a 2D MOP of formula $[\text{Co}_2\text{Cu}_2(\text{mpba})_2(\text{H}_2\text{O})_6] \cdot 6\text{H}_2\text{O}$ with a “brick-wall” structure of (6,3) net topology and metamagnetic behavior.^{6a}

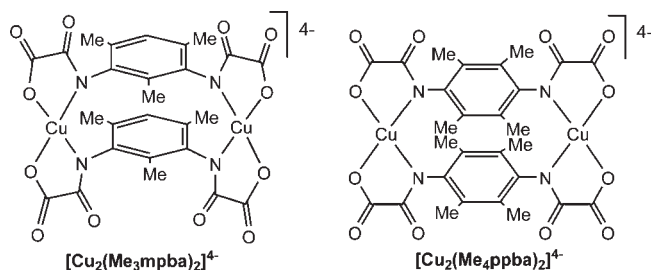
In this Communication, we show that 2D MOPs with such a brick-wall rectangular structure can be obtained when using the related permethylated dicopper(II) analogues $[\text{Cu}_2(\text{Me}_3\text{mpba})_2]^{4-}$ and $[\text{Cu}_2(\text{Me}_4\text{ppba})_2]^{4-}$ [Me_3mpba = 2,4,6-trimethyl-*N,N'*-1,3-phenylenebis(oxamate) and Me_4ppba = 2,3,5,6-tetramethyl-*N,N'*-1,4-phenylenebis(oxamate)] (Chart 1) as tetrakis(bidentate) metalloligands toward bis(chelated) Mn^{II} ions (Scheme 1). Herein we report the synthesis and structural and magnetic characterization of two new manganese(II)–copper(II) 2D MOPs of formulas $[\text{Mn}_2\text{Cu}_2(\text{Me}_3\text{mpba})_2(\text{H}_2\text{O})_6] \cdot 8\text{H}_2\text{O}$ (**1**) and $[\text{Mn}_2\text{Cu}_2(\text{Me}_4\text{ppba})_2(\text{H}_2\text{O})_6] \cdot 8\text{H}_2\text{O}$ (**2**). Compounds **1** and **2** constitute a rare example of control of the spin coupling in MOPs by the topology of the bridging ligand.

Compounds **1** and **2** were both obtained as a pale-green polycrystalline powder and deep-green cubic crystals, respectively, by slow diffusion in an H-shaped tube of aqueous solutions of $\text{Li}_4[\text{Cu}_2\text{L}_2] \cdot n\text{H}_2\text{O}$ [L = Me_3mpba (n = 8) and Me_4ppba (n = 7)] and $\text{Mn}(\text{NO}_3)_2 \cdot 4\text{H}_2\text{O}$ (1:2 molar ratio) at room temperature. The crystal structure of **2** has been solved by single-crystal X-ray diffraction using synchrotron radiation at the BM16 beamline in the ESRF. Our attempts to obtain X-ray quality crystals of **1** were unsuccessful. However, its powder X-ray diffraction pattern was similar to the theoretical one found for the analogue $[\text{Co}_2\text{Cu}_2(\text{mpba})_2(\text{H}_2\text{O})_6] \cdot 6\text{H}_2\text{O}$,^{6a} suggesting thus a common “brick-wall” layer structure (Figure S1 in the Supporting Information).

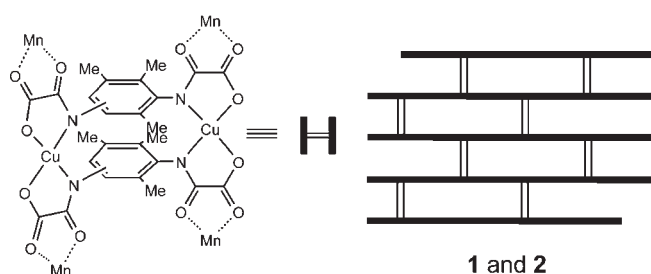
Received: July 7, 2011

Published: August 15, 2011

Chart 1



Scheme 1. Postulated Brick-Wall Rectangular Layer Architecture of the 2D MOPs Resulting from the Self-assembly of Dicopper(II) Metallacyclophane Anionic Complexes and Bis(chelated) Mn^{II} ions



Compound **2** crystallizes in the centrosymmetric $P2_1/n$ space group. The structure of **2** consists of neutral manganese(II)–copper(II) 2D networks, $[\text{Mn}_2\text{Cu}_2(\text{Me}_4\text{ppba})_2(\text{H}_2\text{O})_6]$ (Figures 1 and S2 in the Supporting Information), and free crystallization water molecules. Each dicopper(II) metallacyclophane entity acts as a tetrakis(bidentate) ligand through the carbonyl oxygen atoms of the oxamate ligand atoms toward *cis*-diaquamanganese(II) units, yielding a corrugated brick-wall rectangular layer with a (6,3) net topology growing in the bc plane (Figure 1). There are six copper atoms within each rectangular cell unit of **2**, which occupy the four corners and the middle point of the two long edges of the rectangle, whereas four Mn^{II} ions sit at the one-fourth and three-fourth points of each long edge (Figure 1a). Each $\text{Mn}^{\text{II}}_2\text{Cu}^{\text{II}}_2$ layer of **2** is made up of an extended array of oxamato-bridged zigzag $\text{Mn}^{\text{II}}\text{Cu}^{\text{II}}$ chains running parallel to the crystallographic c axis, which are connected through double para-substituted tetramethylated phenylene spacers (Figure 1b). The shortest intralayer $\text{Cu}\cdots\text{Cu}$ and $\text{Cu}\cdots\text{Mn}$ distances are 7.9606(5) and 5.4105(4)–5.4211(4) Å, respectively.

The Cu(1) atom has a five-coordinated square pyramid (CuN_2O_3), with two amidate nitrogen atoms [$\text{Cu}-\text{N} = 1.9681(14)-1.9869(14)$ Å] and two carboxylate oxygen atoms [$\text{Cu}-\text{O} = 1.9832(12)-1.9833(12)$ Å] from the oxamato groups of the Me_4ppba ligands building the basal plane, with the apical position being occupied by a weakly coordinated water molecule [$\text{Cu}-\text{Ow} = 2.4754(15)$ Å]. On the other hand, the Mn(1) atom is six-coordinated (MnO_6), with two *cis*-coordinated water molecules [$\text{Mn}-\text{Ow} = 2.1439(13)-2.2297(13)$ Å] and four carbonyl oxygen atoms [$\text{Mn}-\text{O} = 2.1415(12)-2.2108(12)$ Å] from two oxamato groups of the Me_4ppba ligands forming distorted octahedral surroundings.

In the crystal lattice of **2**, the adjacent corrugated $\text{Mn}^{\text{II}}_2\text{Cu}^{\text{II}}_2$ layers stack above each other in an eclipsed manner to give an infinite array of interdigitated layers along the [101] direction

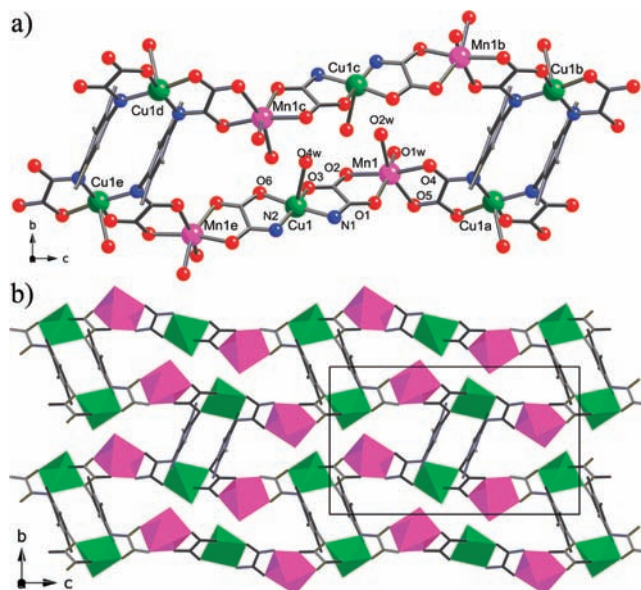


Figure 1. (a) Perspective view of the unit cell of **2** with the atom labeling of the metal environments (hydrogen atoms are omitted for clarity) [symmetry codes: (a) $x + 1/2, -y + 1/2, z + 1/2$; (b) $-x + 1/2, y + 1/2, -z + 1/2$; (c) $-x, -y + 1, -z$; (d) $-x - 1/2, y + 1/2, -z - 1/2$; (e) $x - 1/2, -y + 1/2, z - 1/2$]. (b) Projection view of the 2D neutral network of **2** along the a axis.

(Figure S2a in the Supporting Information). This zipper-type eclipsed packing of neighboring layers leads to small nanopores along the c axis, which are occupied by hydrogen-bonded crystallization water molecules (Figure S2b in the Supporting Information). The shortest interlayer $\text{Cu}\cdots\text{Cu}$, $\text{Cu}\cdots\text{Mn}$, and $\text{Mn}\cdots\text{Mn}$ distances are 7.9616(5), 5.1333(4), and 6.9182(5) Å, respectively.

The direct-current magnetic properties of **1** and **2** in the form of $\chi_{\text{M}}T$ versus T plots (with χ_{M} being the molar magnetic susceptibility per Cu_2Mn_2 unit) are completely different (Figure 2). At room temperature, the values of $\chi_{\text{M}}T$ for **1** and **2** (8.13 and 7.46 $\text{cm}^3 \text{mol}^{-1} \text{K}$, respectively) are lower than those expected for the sum of two Cu^{II} and two Mn^{II} noninteracting ions ($\chi_{\text{M}}T = 9.54 \text{ cm}^3 \text{mol}^{-1} \text{K}$ with $g_{\text{Mn}} = 2.0$, $g_{\text{Cu}} = 2.1$, $S_{\text{Mn}} = 5/2$, and $S_{\text{Cu}} = 1/2$), indicating that a strong antiferromagnetic coupling between Cu^{II} and Mn^{II} ions through the oxamate is operative at room temperature. Upon cooling, $\chi_{\text{M}}T$ for **1** decreases and attains a minimum around 60 K (Figure 2), and then $\chi_{\text{M}}T$ rapidly increases to reach a maximum value of 186 $\text{cm}^3 \text{mol}^{-1} \text{K}$ at about 15.0 K, due to saturation effects. The presence of a $\chi_{\text{M}}T$ minimum for **1** is characteristic of an overall ferrimagnetic behavior resulting from the moderately strong antiferromagnetic interaction between the Mn^{II} and Cu^{II} ions through the oxamate bridge. In this case, it would mask the moderately weak ferromagnetic interaction between the Cu^{II} ions across the double *m*-phenylene spacers via the spin-polarization mechanism,^{7a} as was previously observed in the analogue $[\text{Co}_2\text{-Cu}_2(\text{mpba})_2(\text{H}_2\text{O})_6] \cdot 6\text{H}_2\text{O}$. On the contrary, $\chi_{\text{M}}T$ for **2** continuously decreases upon cooling, and it almost vanishes at 2.0 K, reaching a value of $\chi_{\text{M}}T$ of 0.08 $\text{cm}^3 \text{mol}^{-1} \text{K}$ (Figure 2). This overall antiferromagnetic behavior results from the very strong antiferromagnetic interaction between the Cu^{II} ions across the double *p*-phenylene spacers through the spin-polarization mechanism.^{7b} In this case, it would dominate over

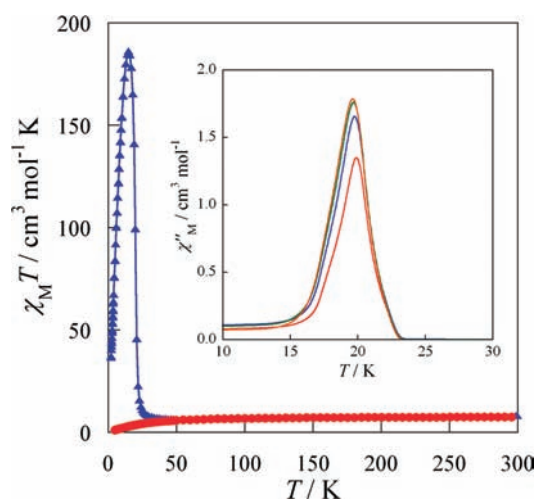


Figure 2. Temperature dependence of $\chi_M T$ for **1** (\blacktriangle) and **2** (\bullet) under an applied magnetic field of 1 T ($T \geq 50$ K) and 100 G ($T < 50$ K). The inset shows the temperature dependence of χ_M'' for **1** with a ± 1.0 G field oscillating at different frequencies (10–1400 Hz). The solid lines are eye guides.

the moderately strong antiferromagnetic interaction between the Mn^{II} and Cu^{II} ions through the oxamate bridge, thus leading to a nonmagnetic ground state for each $\text{Mn}^{\text{II}}_2\text{Cu}^{\text{II}}_2$ layer of **2**. The lack of a maximum of χ_M precludes the occurrence of an antiferromagnetic 3D ordering in the temperature range investigated (2–300 K).

Interestingly, compound **1** undergoes an abrupt paramagnetic-to-ferromagnetic phase transition as revealed by the temperature dependence of the field-cooled magnetization (FCM; Figure S3 in the Supporting Information). The FCM curve, measured by cooling the sample within a small field of 100 G, exhibits an abrupt increase below 25.0 K, thereby suggesting the onset of a 3D ferromagnetic transition resulting from the ferromagnetic interactions between the $\text{Mn}^{\text{II}}_2\text{Cu}^{\text{II}}_2$ layers of **1**. Indeed, the long-range magnetic ordering is confirmed by the alternating-current magnetic properties in the form of the χ_M'' versus T plots (with χ_M'' being the out-of-phase molar magnetic susceptibility per Cu_2Mn_2 unit) at different frequencies (ν) of the ± 1 G oscillating field. Hence, χ_M'' becomes nonzero below 25.0 K, and nonfrequency-dependent maxima are observed at $T_C = 20.0$ K (inset of Figure 2). Indeed, the ferromagnetic nature of the transition is confirmed by the magnetic hysteresis loop at 2.0 K (inset of Figure S3b in the Supporting Information), which is characteristic of a soft magnet, as evidenced by the moderately low value of the coercive field ($H_c = 100$ G).

In conclusion, dicopper(II) metallacyclophanes with permethylated *m*- and *p*-phenylenebis(oxamate) bridging ligands have been used as effective ferro- and antiferromagnetic units, respectively, for the obtention of two novel manganese(II)–copper(II) 2D MOPs with a brick-wall layer structure. The dramatically different magnetic behavior of the resulting 2D MOPs depending on the meta- and para-substitution pattern of the bridging ligand represents thus a successful extension of the concept of ferro- or antiferromagnetic coupling units for control of the spin coupling in coordination polymers on the way toward the rational design of open-framework magnets.

■ ASSOCIATED CONTENT

S Supporting Information. Experimental preparation, analytical and spectroscopic characterization of ligands, dicopper(II) complexes and **1** and **2** X-ray crystallographic data, additional figures (S1–S3), and a crystallographic information file. This material is available free of charge via the Internet at <http://pubs.acs.org>.

■ AUTHOR INFORMATION

Corresponding Author

*E-mail: emilio.pardo@uv.es (E.P.), francisco.lloret@uv.es (F.L.), yves.journaux@upmc.fr (Y.J.).

■ ACKNOWLEDGMENT

This work was supported by the MICINN (Spain; Projects CTQ2010-15364, MAT2010-19681, DPI2010-21103-C04-03, CSD2007-00010, and CSD2006-00015), the Generalitat Valenciana (Spain; Project PROMETEO/2009/108), and the ACIISI-Gobierno Autónomo de Canarias (Spain; Project PIL-2070901 and structuring project NANOMAC) and the MFR and CNRS (France). We also acknowledge the Long Term Project HS3902 of the ESRF, Grenoble, France, for the beamtime assigned. J.F.-S. thanks the Generalitat Valenciana for a doctoral grant. E.P. and J.P. thank the “Juan de la Cierva” (MICINN) and the structuring project NANOMAC, respectively, for postdoctoral contracts.

■ REFERENCES

- (1) Pilkington, M.; Decurtins, S. In *Comprehensive Coordination Chemistry II: From Biology to Nanotechnology*; McCleverty, J. A., Meyer, T. J., Eds.; Elsevier: Oxford, U.K., 2004; Vol. 7, p 177.
- (2) (a) Batten, S. R.; Robson, R. *Angew. Chem., Int. Ed.* **1998**, *37*, 1460. (b) Maspoch, D.; Ruiz-Molina, D.; Veciana, J. *Chem. Soc. Rev.* **2007**, *36*, 770. (c) Janiak, C. *Dalton Trans.* **2003**, 2781. (d) Férey, G. *Chem. Soc. Rev.* **2008**, *37*, 191.
- (3) Verdaguer, M.; Bleuzen, A.; Marvaud, V.; Vaissermann, J.; Seuleiman, M.; Desplanches, C.; Sculler, A.; Train, C.; Garde, R.; Gelly, G.; Lomenech, C.; Rosenman, I.; Veillet, P.; Cartier, C.; Villain, F. *Coord. Chem. Rev.* **1999**, *190*, 1023.
- (4) (a) Kahn, O. *Struct. Bonding (Berlin)* **1987**, *68*, 89. (b) Kahn, O. *Acc. Chem. Res.* **2000**, *33*, 647.
- (5) (a) Pardo, E.; Ruiz-García, R.; Cano, J.; Ottenwaelder, X.; Lescouëzec, R.; Journaux, Y.; Lloret, F.; Julve, M. *Dalton Trans.* **2008**, 2780. (b) Dul, M.-C.; Pardo, E.; Lescouëzec, R.; Journaux, Y.; Ferrando-Soria, J.; Ruiz-García, R.; Cano, J.; Julve, M.; Lloret, F.; Cangussu, D.; Pereira, C. L. M.; Stumpf, H. O.; Pasán, J.; Ruiz-Pérez, C. *Coord. Chem. Rev.* **2010**, *254*, 2281.
- (6) (a) Pereira, C. L. M.; Pedroso, E. F.; Stumpf, H. O.; Novak, M. A.; Ricard, L.; Ruiz-García, R.; Rivière, E.; Journaux, Y. *Angew. Chem., Int. Ed.* **2004**, *43*, 956. (b) Cangussu, D.; Pardo, E.; Dul, M.-C.; Lescouëzec, R.; Herson, P.; Journaux, Y.; Pedroso, E. F.; Pereira, C. L. M.; Stumpf, H. O.; Muñoz, M. C.; Ruiz-García, R.; Cano, J.; Julve, M.; Lloret, F. *Inorg. Chim. Acta* **2008**, *361*, 3394.
- (7) (a) Fernández, I.; Ruiz, R.; Faus, J.; Julve, M.; Lloret, F.; Cano, J.; Ottenwaelder, X.; Journaux, Y.; Muñoz, M. C. *Angew. Chem., Int. Ed.* **2001**, *40*, 3039. (b) Pardo, E.; Faus, J.; Julve, M.; Lloret, F.; Muñoz, M. C.; Cano, J.; Ottenwaelder, X.; Journaux, Y.; Carrasco, R.; Blay, G.; Fernández, I.; Ruiz-García, R. *J. Am. Chem. Soc.* **2003**, *125*, 10770.
- (8) (a) Pardo, E.; Bernot, K.; Julve, M.; Lloret, F.; Cano, J.; Ruiz-García, R.; Delgado, F. S.; Ruiz-Pérez, C.; Ottenwaelder, X.; Journaux, Y. *Inorg. Chem.* **2004**, *43*, 2768. (b) Pardo, E.; Ruiz-García, R.; Lloret, F.; Julve, M.; Cano, J.; Pasán, J.; Ruiz-Pérez, C.; Filali, Y.; Chamoreau, L. M.; Journaux, Y. *Inorg. Chem.* **2007**, *46*, 4504.